ISSN: 2181-3337 | SCIENTISTS.UZ VOLUME 5 ISSUE 7 JULY 2026

MODEL-BASED ASSESSMENT OF A 60 W MONOCRYSTALLINE PHOTOVOLTAIC MODULE AND TWO THREE-MODULE CONFIGURATIONS UNDER HOT-SUMMER CONDITIONS IN TERMEZ, UZBEKISTAN

Yuldoshov Boysori[1], **Kholmuminov Asadbek**[2]
[1]Termez State University, Uzbekistan;
[2]Specialized School of Jarkurgan District, Uzbekistan;
Manuscript type: modeling and simulation study

DOI: 10.67620/sai.57a0008

ABSTRACT

This study presents a reproducible model-based assessment of a representative 60 W monocrystalline photovoltaic module and two 180 W three-module array configurations under a prescribed hot-summer day in Termez, Uzbekistan. Solar position was calculated at 15-minute resolution for 13 July 2026 using the site coordinates (37.22° N, 67.28° E) and local civil time (UTC+5). Clear-sky global horizontal irradiance was estimated with the Haurwitz model, separated into direct and diffuse components using the Erbs correlation, and transposed to tilted planes using an isotropic-sky formulation. Module temperature was calculated with the NOCT-SAM model, and DC power was estimated using a linear temperature-corrected power relationship. System 1 comprised three co-planar modules tilted 14° and facing south. System 2 comprised one east-facing, one south-facing, and one west-facing module, all tilted 14°; optical concentration and inter-module reflection were not assumed. The model placed solar noon at 12:36 local time and the maximum south-facing plane-of-array irradiance at 12:30, thereby maintaining consistency between solar geometry and irradiance. The south-facing module reached 74.5°C and a maximum DC power of 49.4 W. Daily DC energy was 428.1 Wh per south-facing module, 1284.3 Wh for System 1, and 1275.4 Wh for System 2. The east-south-west arrangement reduced the array peak by 3.0% and increased morning and evening energy by 4.5% and 8.0%, respectively, but reduced total daily energy by 0.70%. The results show that orientation diversification can flatten the production profile without necessarily increasing daily energy. Because the analysis uses a clear-sky model, a prescribed temperature profile, and constant wind speed, field measurements are required before site-specific performance claims are made.

ACCEPTED

07.08.26

Keywords: *photovoltaic module; solar geometry; plane-of-array irradiance; module temperature; NOCT model; azimuth diversification; Termez.*

CC BY

1. Introduction

Photovoltaic (PV) output is governed jointly by irradiance, cell temperature, module characteristics, and array orientation. Standard test conditions provide a common nameplate reference, but they do not represent the thermal environment of an operating module. In hot and highly insolated climates, cell

temperature can rise several tens of degrees above ambient temperature, reducing voltage and maximum power even when incident irradiance is high. Consequently, a technically useful assessment must treat solar geometry, plane-of-array irradiance, module temperature, and electrical conversion as a linked calculation rather than as independent quantities (Dobos, 2014; Duffie & Beckman, 2013; Gilman et al., 2018).

Termez is located in southern Uzbekistan near 37° N and experiences hot summer conditions. The combination of high solar elevation and high ambient temperature makes the region a relevant case for evaluating the thermal derating of crystalline-silicon PV modules. The original version of this study compared a co-planar three-module array with an angled arrangement, but it mixed modeled and measured terminology, did not provide a reproducible irradiance time base, and attributed a reflector benefit without an optical model. The present revision resolves those problems by treating the work explicitly as a simulation, defining every input and equation, aligning irradiance with solar noon, integrating energy with the actual time step, and excluding unmodeled reflection effects.

The objectives are to:

calculate a physically consistent 15-minute clear-sky irradiance profile for Termez;

estimate the operating temperature, short-circuit current, open-circuit voltage, and DC power of a representative 60 W module;

compare a co-planar south-facing array with an east-south-west azimuth-diversified array; and

quantify the sensitivity of the result to wind speed, NOCT, temperature coefficient, and irradiance uncertainty.

2. Materials and methods

2.1 Study site, time basis, and study design

The site coordinates were latitude 37.22° N and longitude 67.28° E. Calculations were performed for 13 July 2026 at 15-minute intervals in local civil time (UTC+5). The local standard meridian was 75° E. The equation-of-time and longitude correction gave a calculated solar noon of 12:36. Sunrise and sunset were approximately 05:25 and 19:47, respectively. Solar angles were evaluated using standard astronomical relationships consistent with the NREL solar-position framework (Reda & Andreas, 2008).



Figure 1. A monocrystalline silicon photovoltaic panel with a nominal power of 60W

The study is a deterministic clear-sky simulation. The ambient-temperature series was prescribed to reproduce the hot-day boundary condition reported in the source manuscript, ranging from 27.3°C before sunrise to 42.5°C in the afternoon. The previously missing 12:45 value was inserted by time interpolation. Wind speed at 10 m was set to 1.1 m s^{-1} for the baseline case and varied in sensitivity analysis. The temperature series is not presented as a meteorological observation; therefore, the results are comparative model outputs rather than validated site measurements.

ISSN: 2181-3337 | SCIENTISTS.UZ

Parameter	Baseline value	Role in model
Latitude / longitude	37.22° N / 67.28° E	Solar position
Date and time step	13 July 2026; 15 min	Daily clear-sky case
Time standard	UTC+5; standard meridian 75° E	Civil-to-solar-time conversion
Ambient temperature	27.3–42.5°C; prescribed profile	Thermal boundary condition
Wind speed at 10 m	1.1 m s^{-1}	Baseline module cooling
Ground albedo	0.20	Ground-reflected irradiance
Array tilt	14°	All modules

Table 1. Site and baseline boundary conditions.

2.2 Solar position and clear-sky irradiance

The clear-sky global horizontal irradiance (GHI) was estimated with the Haurwitz relationship (Haurwitz, 1945). The model is intentionally simple and is suitable for a transparent comparative study; it does not represent aerosol, water-vapour, dust, or cloud variability specific to an individual day.

$$GHI_{cs} = 1098 \cos(\theta_z) \exp[-0.059 / \cos(\theta_z)] \quad (1)$$

where θ_z is the solar zenith angle. GHI was decomposed into diffuse horizontal irradiance (DHI) and direct normal irradiance (DNI) using the hourly diffuse-fraction correlation of Erbs et al. (1982).

$$k_t = GHI_{cs} / (I_{0n} \cos \theta_z), \quad DHI = k_d GHI_{cs}, \quad DNI = (GHI_{cs} - DHI) / \cos \theta_z \quad (2)$$

The plane-of-array irradiance for a surface with tilt β and incidence angle θ_i was calculated with the isotropic-sky transposition model (Duffie & Beckman, 2013; Klein, 1979).

$$G_{POA} = DNI \max(\cos \theta_i, 0) + DHI(1 + \cos \beta)/2 + \rho_g GHI(1 - \cos \beta)/2 \quad (3)$$

The use of $\max(\cos \theta_i, 0)$ prevents beam irradiance from being assigned to the rear surface. The ground-reflection term used $\rho_g = 0.20$. No optical concentration, inter-module reflection, or bifacial gain was included.

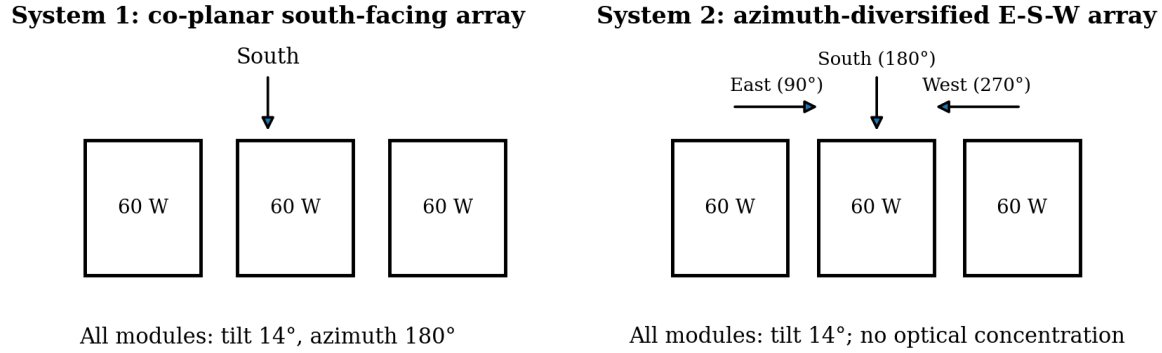


Figure 1. Modeled three-module array configurations. The drawing is schematic; all modules have a 14° tilt.

ISSN: 2181-3337 | SCIENTISTS.UZ

2.3 Reference PV module and temperature model

A representative 36-cell monocrystalline module was defined from the electrical values used in the source manuscript. Because no manufacturer and model number were supplied, the parameters in Table 2 are model inputs rather than a certified datasheet. This distinction prevents the results from being attributed to a specific commercial module.

Parameter	Symbol	Value
Maximum power at STC	P_{STC}	60 W
Open-circuit voltage at STC	$V_{oc,STC}$	22.0 V
Short-circuit current at STC	$I_{sc,STC}$	3.66 A
Power temperature coefficient	γ_P	−0.40% °C⁻¹
Current temperature coefficient	α_I	+0.05% °C⁻¹
Voltage temperature coefficient	β_V	−0.30% °C⁻¹ of $V_{oc,STC}$
Nominal operating cell temperature	NOCT	45°C
Reference efficiency	η_{ref}	0.12
Effective transmittance–absorptance	$\tau\alpha$	0.90
Cells in series	N_s	36

Table 2. Reference module parameters used in the simulation.

Module temperature was evaluated with the NOCT formulation implemented in the NREL System Advisor Model (SAM; Gilman et al., 2018). International Electrotechnical Commission (IEC) standard 61853-2 defines procedures for module operating-temperature measurements, whereas IEC 61215 addresses design qualification and is not used here as the source of the NOCT calculation (IEC, 2016, 2021b). For an open-rack installation, the adjusted NOCT equals the input NOCT.

$$T_c = T_a + (G_{POA}/800)(NOCT - 20)(1 - \eta_{ref}/\tau\alpha) \cdot 9.5/(5.7 + 3.8v_{w,adj}) \quad (4)$$

$$v_{w,adj} = 0.51v_w \quad (5)$$

2.4 Electrical model and energy integration

The maximum-power DC output was calculated with the linear irradiance-and-temperature relationship used in simplified PV energy models such as PVWatts (Dobos, 2014).

$$P_{dc} = P_{STC}\,(G_{POA}/1000)[1 + \gamma_P(T_c - 25)] \quad (6)$$

For diagnostic reporting, short-circuit current and open-circuit voltage were estimated as follows:

$$I_{sc} = I_{sc,STC}\,(G_{POA}/1000)[1 + \alpha_I(T_c - 25)] \quad (7)$$

$$V_{oc} = V_{oc,STC} + \beta_V(T_c - 25) + N_{snk}(T_c + 273.15)q^{-1}\ln(G_{POA}/1000) \quad (8)$$

Equation (8) was applied only for $G_{POA} \geq 20$ W m^{-2}, with ideality factor $n = 1.2$. It is a diagnostic semi-empirical expression and not a substitute for a fitted single-diode model. Daily energy was calculated by trapezoidal integration at the actual 0.25 h time step:

ISSN: 2181-3337 | SCIENTISTS.UZ

$$E = \Sigma [(P_j + P_{j+1})/2] \Delta t \quad (9)$$

2.5 Array configurations

System 1 contained three identical modules, each tilted 14° and facing south (azimuth 180°). System 2 contained three identical modules at the same tilt, facing east (90°), south (180°), and west (270°). Module-level maximum-power tracking was assumed, so the three module powers were added without parallel mismatch loss. This assumption isolates the geometric effect; a shared MPPT could produce additional mismatch and should be considered in hardware design.

The revised System 2 intentionally excludes the earlier "reflector effect." Conventional PV laminates are primarily absorptive, and any multiple-reflection benefit would require measured reflectance, module spacing, shading geometry, view factors, and optical ray tracing. Those inputs were unavailable and were therefore not fabricated.

2.6 Sensitivity analysis

One-at-a-time sensitivity cases varied wind speed (0.5–4.0 m s^{-1}), γ_P (−0.35 to −0.45% $°C^{-1}$), NOCT (43–47°C), and all irradiance components (±5%). These ranges test whether the comparative result is robust to the principal prescribed inputs.

3. Results

3.1 Solar geometry and plane-of-array irradiance

The model gave solar noon at approximately 12:36 local time. The maximum clear-sky GHI was 995.5 W m^{-2} at 12:30; the south-facing plane-of-array irradiance reached 1026.6 W m^{-2} at 12:30. The coincidence of the irradiance maximum with solar noon corrects the earlier timing inconsistency. Because the tilt was only 14°, the east- and west-facing plane-of-array daily irradiances remained close to the south-facing value, but their intraday profiles shifted toward morning and afternoon, respectively.

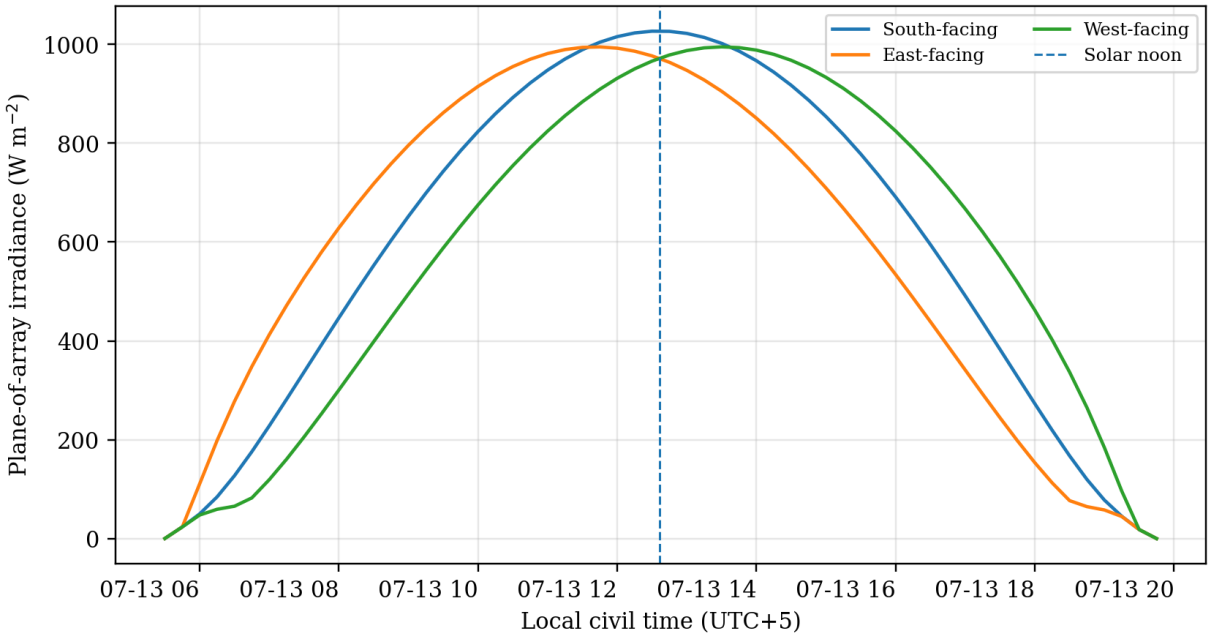


Figure 2. Clear-sky plane-of-array irradiance for the three modeled azimuths.

3.2 Module temperature and electrical parameters

For the south-facing module, the modeled cell temperature reached 74.5°C at 12:30, compared with a maximum ambient temperature of 42.5°C at 14:45. At the maximum-power time, I_{sc} was 3.85 A, V_{oc} was 18.77 V, and DC power was 49.39 W. Thus, an irradiance slightly above 1000 W m^{-2} did not produce the 60 W nameplate value because the cell temperature was about 49.5°C above the STC reference temperature. This is reversible thermal derating, not evidence of permanent material degradation.

ISSN: 2181-3337 | SCIENTISTS.UZ

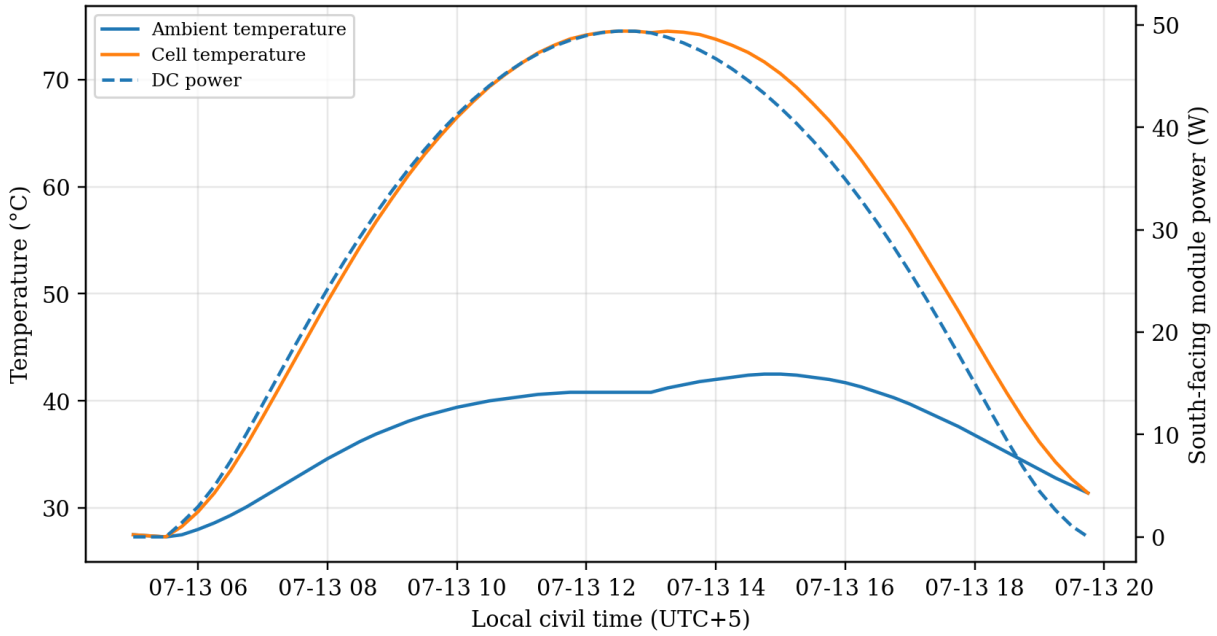


Figure 3. Ambient temperature, modeled cell temperature, and DC power of the south-facing module.

3.3 Comparison of the two array configurations

Metric	South-facing module	System 1	System 2
Nominal DC capacity	60 W	180 W	180 W
Peak modeled DC power	49.39 W	148.18 W	143.71 W
Daily modeled DC energy	428.1 Wh	1284.3 Wh	1275.4 Wh
Daily energy relative to System 1	—	Reference	-0.70%
Morning energy change (to 09:00)	—	Reference	+4.5%
Evening energy change (from 17:00)	—	Reference	+8.0%

Table 3. Principal electrical results for the baseline case.

System 1 generated 1284.3 Wh, whereas System 2 generated 1275.4 Wh, a difference of -0.70%. System 2 reduced peak power by 3.0% and redistributed energy toward the shoulders of the day: energy increased by 4.5% up to 09:00 and by 8.0% after 17:00, while the central part of the day decreased by approximately 2.5%. The configuration therefore flattened the production profile, but it did not provide a daily-energy advantage under the modeled clear-sky conditions.

ISSN: 2181-3337 | SCIENTISTS.UZ

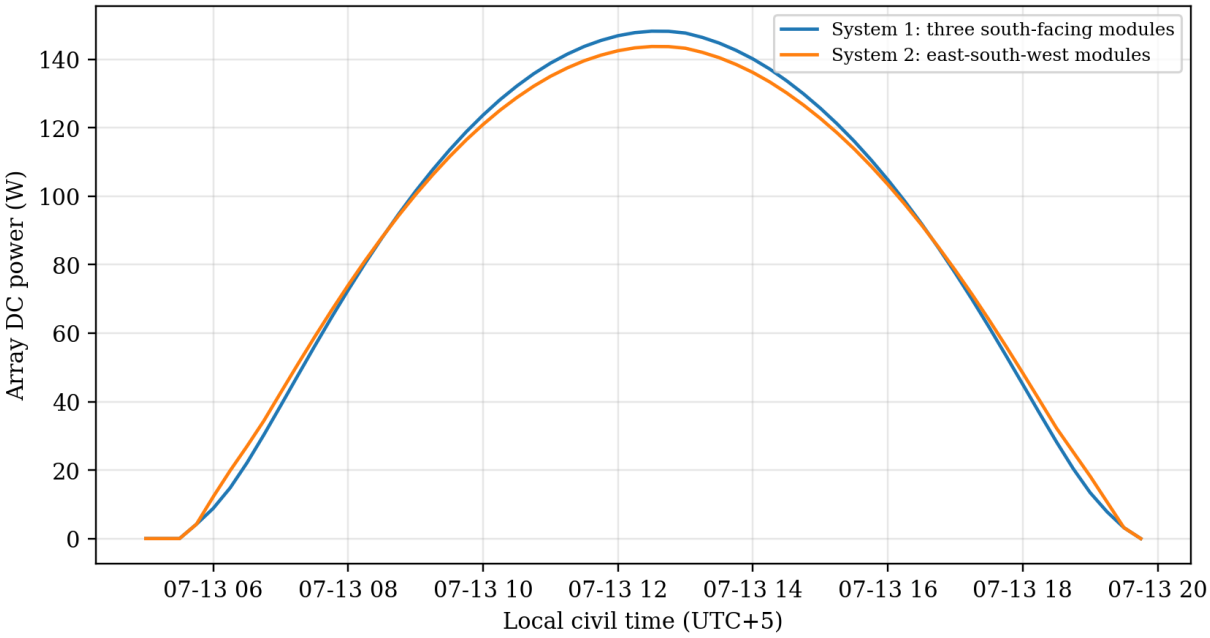


Figure 4. Modeled DC power profiles of the two 180 W array configurations.

3.4 Sensitivity analysis

Parameter	Value	System 1 (Wh)	System 2 (Wh)	System 2 difference
Wind speed at 10 m (m/s)	0.5	1256.3	1248.0	-0.66%
Wind speed at 10 m (m/s)	1.1	1284.3	1275.4	-0.70%
Wind speed at 10 m (m/s)	2	1313.6	1304.0	-0.73%
Wind speed at 10 m (m/s)	4	1351.5	1340.9	-0.78%
Power temperature coefficient (%/°C)	-0.35	1315.8	1306.2	-0.73%
Power temperature coefficient (%/°C)	-0.4	1284.3	1275.4	-0.70%
Power temperature coefficient (%/°C)	-0.45	1252.8	1244.6	-0.66%
NOCT (°C)	43	1297.2	1287.9	-0.71%
NOCT (°C)	45	1284.3	1275.4	-0.70%
NOCT (°C)	47	1271.5	1262.8	-0.68%
Irradiance multiplier	0.95	1227.7	1219.1	-0.71%
Irradiance multiplier	1	1284.3	1275.4	-0.70%
Irradiance multiplier	1.05	1340.1	1330.9	-0.68%

Table 4. One-at-a-time sensitivity results.

ISSN: 2181-3337 | SCIENTISTS.UZ

Absolute energy changed materially with wind speed, temperature coefficient, NOCT, and irradiance level, as expected. However, the relative daily-energy difference between the two configurations remained close to −0.7% in all tested cases. This stability occurs because the two systems use the same module model and differ mainly in azimuth. Accordingly, the conclusion that the east-south-west arrangement flattens rather than increases the clear-sky daily yield is robust within the stated assumptions.

4. Discussion

4.1 Thermal derating under hot conditions

The modeled cell temperature exceeded 70°C near solar noon. IEC 61215-1-1 notes that higher-temperature qualification may be relevant in climates where the 98th-percentile operating temperature exceeds 70°C (IEC, 2021a). The present study does not establish that percentile because it covers one prescribed day, but it illustrates why module selection, rear ventilation, mounting stand-off, and measured temperature coefficients matter in hot climates. The decrease from 60 W nameplate power to approximately 49 W at peak modeled conditions follows from the combined temperature and irradiance terms in Equation (6); it should be described as operating derating rather than degradation.

4.2 Meaning of the orientation comparison

A low 14° tilt limits the daily-energy penalty associated with east and west azimuths. Consequently, System 2 retained almost all of the co-planar array's daily energy while lowering the midday peak and increasing shoulder production. This type of profile shaping can be useful where local demand is higher in the morning or late afternoon, where inverter clipping is a concern, or where a smoother output profile has operational value. It does not imply a higher conversion efficiency: the result is a temporal redistribution of incident radiation.

The calculation also demonstrates why a reflector claim cannot be based solely on array geometry. Any optical enhancement would depend on front-glass reflectance, incidence angle, module spacing, the fraction of reflected light intercepted by another module, shading, and the electrical response of the illuminated cells. A valid reflector study would require measured bidirectional optical properties or validated ray tracing coupled to a cell-level mismatch model.

4.3 Comparison with the unrevised calculation

The revised model corrects four central issues: (i) the work is consistently identified as simulation rather than measurement; (ii) solar noon and the irradiance maximum are aligned through an explicit civil-to-solar-time conversion; (iii) the 12:45 interval is present and energy is integrated by timestamp; and (iv) the system comparison uses explicit azimuths and excludes unsupported reflection. These changes alter the scientific conclusion. The modeled azimuth-diversified system does not produce a 12% daily-energy gain; instead, it produces a nearly equal daily yield with a broader output profile.

5. Limitations and future validation

The following limitations define the scope of the conclusions:

The Haurwitz clear-sky model is an empirical reference and does not include day-specific aerosols, dust, water vapour, or clouds.

The ambient-temperature curve is a prescribed hot-day boundary condition, not a verified observation for 13 July 2026.

Wind speed is constant in the baseline case, and the NOCT model does not resolve transient thermal inertia.

The module is representative because no manufacturer datasheet was available; a single-diode model could improve electrical accuracy.

Module-level MPPT was assumed. Shared-MPPT wiring may introduce mismatch losses for differently oriented modules.

Soiling, spectral effects, incidence-angle modifiers, cable loss, inverter loss, shading, and reflection between modules were excluded.

ISSN: 2181-3337 | SCIENTISTS.UZ

Future work should collect synchronized plane-of-array irradiance, ambient temperature, rear-surface or cell temperature, wind speed, and module I–V data for both configurations. Sensors should be time-synchronized in local civil time, and the raw dataset, calibration certificates, data-processing code, and uncertainty budget should be published. Experimental performance should then be evaluated using measured energy, normalized yield, model bias, mean absolute error, and root-mean-square error.

6. Conclusions

This paper provides a fully specified simulation of a representative 60 W monocrystalline PV module and two 180 W array configurations under prescribed hot-summer conditions in Termez. The corrected solar-time calculation placed solar noon at 12:36 and the maximum south-facing irradiance at 12:30. The modeled module temperature reached 74.5°C, limiting the maximum 60 W module output to 49.4 W despite plane-of-array irradiance above 1000 W m^{-2}.

Three co-planar south-facing modules generated 1284.3 Wh in the modeled day. The east-south-west array generated 1275.4 Wh, 0.70% less, while reducing peak power by 3.0% and increasing morning and evening energy. The primary benefit of the diversified arrangement was therefore profile flattening, not higher daily energy. Claims of reflector-assisted gain are not supported without an explicit optical model and experimental validation.

The main practical conclusion is that hot-climate PV assessment must combine correct solar geometry with temperature-aware electrical modeling. The present results are suitable as a transparent modeling baseline; they should not be presented as measured site performance until validated by field data.

Declarations

Author contributions. B.Y.: conceptualization, methodology, supervision, and manuscript review. A.K.: calculation implementation, data organization, visualization, and draft preparation. Both authors approved the final manuscript.

Conflict of interest. The authors declare no conflict of interest.

Funding. No external funding was reported for this modeling study.

Data and code availability. All model parameters, equations, and the complete 15-minute baseline dataset are provided in this paper and Appendix A. The calculations can be reproduced using the stated equations in any numerical software.

Use of human or animal subjects. Not applicable.

REFERENCES

1. Dobos, A. P. (2014). *PVWatts version 5 manual* (NREL/TP-6A20-62641). National Renewable Energy Laboratory. https://doi.org/10.2172/1158421
2. Duffie, J. A., & Beckman, W. A. (2013). *Solar engineering of thermal processes* (4th ed.). Wiley. https://doi.org/10.1002/9781118671603
3. Erbs, D. G., Klein, S. A., & Duffie, J. A. (1982). Estimation of the diffuse radiation fraction for hourly, daily, and monthly-average global radiation. *Solar Energy, 28*(4), 293–302. https://doi.org/10.1016/0038-092X(82)90302-4
4. Gilman, P., Dobos, A., DiOrio, N., Freeman, J., Janzou, S., & Ryberg, D. (2018). *SAM photovoltaic model technical reference update* (NREL/TP-6A20-67399). National Renewable Energy Laboratory. https://doi.org/10.2172/1429291
5. Haurwitz, B. (1945). Insolation in relation to cloudiness and cloud density. *Journal of Meteorology, 2*(3), 154–166. https://doi.org/10.1175/1520-0469(1945)002<0154:IIRTCA>2.0.CO;2
6. International Electrotechnical Commission. (2016). *Photovoltaic (PV) module performance testing and energy rating—Part 2: Spectral responsivity, incidence angle and module operating temperature measurements* (IEC 61853-2:2016).

7. International Electrotechnical Commission. (2021a). *Terrestrial photovoltaic (PV) modules—Design qualification and type approval—Part 1-1: Special requirements for testing of crystalline silicon photovoltaic (PV) modules* (IEC 61215-1-1:2021).
8. International Electrotechnical Commission. (2021b). *Terrestrial photovoltaic (PV) modules—Design qualification and type approval—Part 1: Test requirements* (IEC 61215-1:2021).
9. Klein, S. A. (1979). Calculation of monthly average insolation on tilted surfaces. *Solar Energy, 19*(4), 325–329. https://doi.org/10.1016/0038-092X(77)90001-9
10. Reda, I., & Andreas, A. (2008). *Solar position algorithm for solar radiation applications* (Rev.; NREL/TP-560-34302). National Renewable Energy Laboratory. https://doi.org/10.2172/15003974

ISSN: 2181-3337 | SCIENTISTS.UZ